A Thermodynamic Interpretation of the Stimulated Raman Signature of an Action Potential in a Neuron

Shamit Shrivastava[1,2*], Hyeon Jeong Lee[3,4], and Ji-Xin Cheng[3,4]

1. *Department of Engineering Science, University of Oxford, Oxford, UK*
2. *Institute for Sound and Light, Rosalind Franklin Institute, Harwell, UK*
3. *Department of Biomedical Engineering, Boston University, MA USA*
4. *Department of Electrical and Computer Engineering, Boston University, MA USA*

*Corresponding Author: shamit.shrivastava@eng.ox.ac.uk

Draft: 20th April 2020

Abstract

It has previously been suggested that the plasma membrane condenses and melts reversibly during an action potential in a neuron. If true it has fundamental consequences for our understanding of the regulation of biological functions during an action potential. It has long been known that the electrical dipoles in the neuronal membrane reorient during an action potential, observed through a variety of optical methods. However, this information has been insufficient to confirm if and how the collective thermodynamic state of the neuronal membrane changes during an action potential. Here, we show that hyperspectral stimulated Raman spectroscopy can resolve the thermodynamic state of the plasma membrane in a single neuron during an action potential. Based on these measurements we provide the first evidence that the neuronal membrane condenses during the de-polarisation phase, while the membrane melts during the polarisation and hyperpolarisation phase.

Statement of Significance

While action-potentials can be measured using a variety of methods, none of these methods have been able to provide sufficient information to characterise the collective thermodynamic state of the membrane during an action-potential. Therefore, new tools are required to satisfactorily resolve the fundamental nature of the phenomenon, i.e. does the wave-front propagates irreversibly/diffusively as in the burning of a fuse, or reversibly/elastically as in the propagation of sound. It has been postulated that if action-potentials indeed propagate elastically, then the membrane must undergo a localised condensation during the action-potential. This article confirms and quantifies the condensation of the membrane during an action-potential based on time-resolved changes in the Raman band at 2930 cm^{-1}, also known as the "melting-marker".

Introduction

Exciting a neuron causes all – or – none voltage spikes that can be measured between two electrodes that are placed across the neuronal membrane. These voltage spikes are known as action potentials and are generated in the neuronal membrane(1). The present understanding of the phenomenon of action potentials originated from extensive empirical studies on the electrochemical properties of nerves(2). However, these spikes can also be measured using nonelectrical methods such as changes in displacements(1, 3), turbidity, birefringence(4), fluorescence(1, 5), magnetic field(6), force(1), as well as temperature(1, 7). While these nonelectrical aspects of the action potential are well known, they are believed to be non –

essential for the biological functions of the action potential. Moreover, the observations themselves are explained as epiphenomenon driven by the voltage spikes using empirical coupling coefficients(8). However, from a material perspective, changes in temperature and displacement are fundamental to the understanding of any spike or wave propagation phenomenon, as required by the conservation laws of mass, momentum, and energy(9). For example, the present understanding describes the action potential as a purely dissipative phenomenon in analogy to the burning of a fuse where the wavefront propagates as a result of irreversible and diffusive mass (ion) transfer. Hodgkin described in 1964, "The invariance of the action potential arises because the energy used in propagation does not come from stimulus but is released by the nerve fibre along its length. In this respect nervous conduction resembles the burning of a fuse of gunpowder and is unlike current in an electrical cable"(10). Disregarding the "energy of the stimulus" is equivalent to disregarding the role of reversible momentum transfer as seen, for instance, during a sound wave propagation. However, heat studies in nerves indicate that an action potentials is a substantially reversible process(7, 11). As a result, the electrochemical understanding of action potentials that ignores the role of heat and momentum transfer during the action potential has long been debated(1, 12, 13).

Recent research has brought the thermodynamic underpinnings of the phenomenon at the centre of this debate by describing the nerve impulse as a material wave that propagates as a localized condensation of the membrane(14, 15). The theory incorporates all the non-electrical aspects of the nerve impulse as default thermodynamic couplings and explains the observed reversible heating and cooling as a default consequence of adiabatic compression and rarefaction of the medium during pulse propagation. A particular prediction of the theory is a change in the state of the matter so significant that the membrane's thermodynamic susceptibilities, such as heat capacity and compressibility, change significantly. Such significant changes in the compressibility are observed during thermotropic transitions in biological(16, 17) as well as artificial lipid interfaces(18). Under such conditions the nonlinear properties of the action potentials, such as all – or – none excitation and annihilation of pulses upon collision, are also shown by compression waves in artificial lipid films(19, 20), indicating that the "invariance of action potentials" can arise also from momentum transfer. Therefore, the theory predicts a condensation (freezing) of the membrane during an action potential as it depolarises and a rarefaction (melting) as it polarises again. The hyperpolarisation is then a consequence of the inertia as the membrane relaxes(19, 21). However, a direct measurement of the membrane state to confirm its freezing during an action potential has remained elusive. Here, by observing the changes in a signature Raman peak of the plasma membrane that changes only during melting, we confirm that the thermodynamic state of the membranes changes significantly, as in a phase transition, during an action potential in a single neuron.

Measuring thermodynamic state changes from light-matter interaction

Optical methods have a long history in measuring physical changes in the membrane during an action potential(5, 22). The electromagnetic nature of light allows probing the changes in the electric field around the dipoles, either extrinsic or intrinsic to the membrane, due to changes in membrane potential. Thus changes in optical signals, in general, can be easily mapped to changes in membrane potentials, which form the basis for many important methods for studying action potentials. However, such light-matter interactions do not lie outside the purview of thermodynamics(23, 24), and the properties of light can indeed be used as thermodynamic observables of the system that they interact with(25, 26).

When photons interact with a material, a small fraction of their population changes its wavelength due to the second-order effects of the thermal fluctuations in the material(27). These perturbed photons lie on a spectrum and the frequency distribution of the photons directly represents the partition of thermal energy among the conformational states. Raman and infrared spectroscopy-based methods are well known to characterize the conformational state of artificial and biological membranes (28–30). Here, we exploit this relationship to obtain new insights into the nature of physical changes in neuronal membranes during an action potential.

We start with fact that the entropy of a membrane complex can be written as a thermodynamic function of the form $S \equiv S(x_i)$(26, 31), where $x_i's$ are the extensive observables of the system that can be measured experimentally, e.g. volume, number of charges, number of photons, enthalpy, etc.

At equilibrium, the entropy is maximum, therefore the first derivative of the entropy potential $dS(x_i) = 0$. Using this the Taylor expansion of the entropy potential can be written as:

$$S - S_0 = \sum_{i,j} \frac{\partial^2 S}{\partial x_i \partial x_j} \delta x_i \delta x_j \quad (1)$$

The equation is also valid during non-equilibrium processes(32, 33) under the assumption of local equilibrium where the state variables are defined spatio-temporally. Using eq. (1) and the inversion of Boltzmann principle $w = e^{S/k}$ it can be shown that various observables must be coupled by the relation

$$\langle \Delta x_i, \Delta x_j \rangle \propto -\left(\frac{\partial^2 S}{\partial x_i \partial x_j}\right)^{-1} \quad (2)$$

So how do these equations help us in understanding thermodynamic changes in membranes using Raman spectroscopy? If the Raman spectrum is represented by the function I_n, i.e. the number of photons at wavenumber n, then as per the above, we propose the ansatz that the entropy of a complex membrane can also be written as $S = S(I_n, x_i)$ (23, 34). Since all the arguments of the function are experimentally measurable, the function provides a general basis for designing experiments, where x_i are chosen depending on the phenomenon of interest. For example, I_n can be measured as a function of temperature, T, and in that case eq.(2) gives;

$$\langle \Delta I_n, \Delta H \rangle \propto -\left(\frac{\partial^2 S}{\partial H \partial I_n}\right)^{-1} = -\left(\frac{\partial}{\partial I_n}\frac{\partial S}{\partial H}\right)^{-1} = \kappa T^2 \left(\frac{\partial I_n}{\partial T}\right) \quad (3)$$

i.e. small changes in intensity at a given wavenumber ΔI_n for a given change in the total enthalpy of the system, ΔH are required to obey eq.(3) as per the second law of thermodynamics. Here κ is the Boltzmann constant and $\left(\frac{\partial I_n}{\partial T}\right)$ represents the derivative of the experimentally measured function $I_n(T)$. Therefore, for conformational changes that occur during a process in the membrane, as observed from ΔI_n, an equivalent enthalpy change can be estimated from Eq. (3). Similarly, I_n can also be investigated as a function of pressure or electric field to reflect changes in volume or membrane potential.

State changes during voltage-clamped experiments

A voltage-clamp experiment can be assumed to be a constant temperature or isothermal experiment (at the temperature of the sample chamber), while other variables are free to adjust (e.g. membrane pressure or interfacial pH). Then the changes in state as per eq. (2) are due to

changes in the electrical field applied to the membrane. Recently, Lee and Cheng reported spatially and temporally resolved I_n measurements on single neurons using stimulated Raman scattering (SRS) spectroscopy(35). As discussed above, the data was interpreted by studying I_n as a function of membrane potential, showing that structural changes in a single neuron can be resolved during an action potential based on observed ΔI_n. Figure 1c shows a typical SRS spectrum of a neuron at the resting potential, I_n for $n \in [2800,3000] cm^{-1}$ indicating the strongest contribution from a peak at $2930\ cm^{-1}$. Figure 1e shows the changes in the SRS spectra ΔI_n measured during somatic voltage clamp of a neuron $(-80\ mV\ to + 30\ mV)$ with respect to the resting potential of $-60mV$. Thus, the intensity of $2930\ cm^{-1}$ peak decreases in response to membrane depolarisation and increase upon hyperpolarisation.

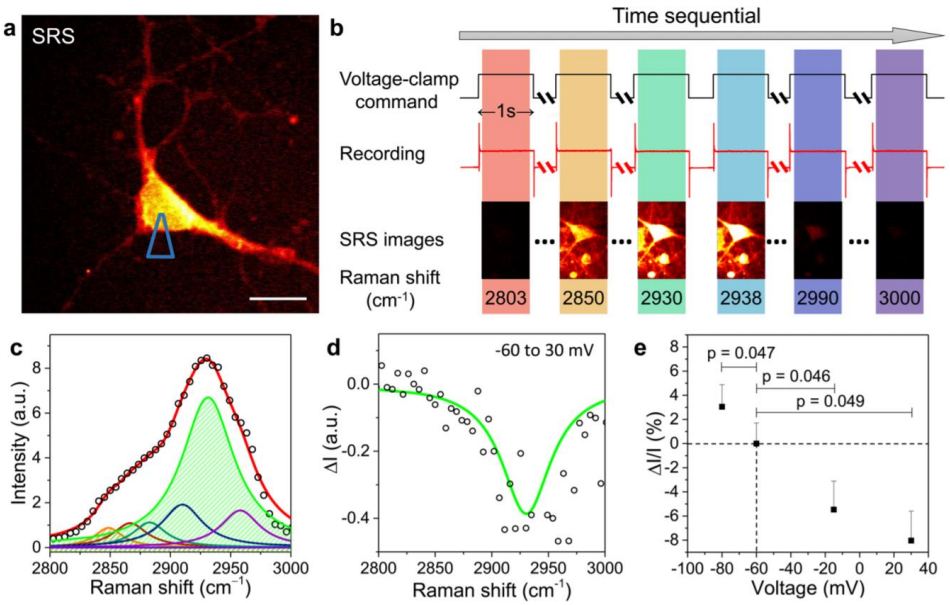

Figure 1 (a) SRS image of a patched neuron with micropipette position indicated. Scale bar: 10 μm. (b) Schematic of hyperspectral SRS imaging of neurons while holding different potentials. (c) Representative SRS spectrum of a patched neuron (dot), fitted using seven Lorentzian (colored lines) with major contributing bands filled, 2850 (orange) and 2930 cm^{-1} (green). Red: cumulative fitted curve. (d) SRS spectral change, ΔI (dots), of the neuron from −60 to +30 mV with fitted curve (line). (e) Percentage changes of SRS intensity (ΔI/I) of neurons at 2930 cm^{-1} at various membrane potentials. Error bars: + standard error of the mean (SEM). Reprinted (adapted) with permission from (J. Phys. Chem. Lett. 2017, 8, 9, 1932-1936). Copyright (2017) American Chemical Society

Here, we provide a mesoscopic and thermodynamic interpretation of these changes based on eq. (3). To do that, it is important to remind ourselves that eq. (3) does not assume the underlying molecular structure of the membrane, i.e. it is invariant of the molecular origin of Raman signal which could be due to any protein, lipids, ion, etc. This invariance provides us with means to refer to model systems for simulating ΔI_n (as observed in real neurons) and derive new insights from it. In this sense, changes in I_{2930} as a function of the state has been measured in a variety of artificial as well as biological membranes. Both in lipids and proteins, the band represents a "melting marker" as the peak at $2930\ cm^{-1}$ appears in difference spectra ΔI_n only when the corresponding state change involves a cooperative thermotropic transition or melting(36). These studies(37–40) usually measure intensity around $2930\ cm^{-1}$ relative to

intensity at another wavenumber, which provides an internal reference that removes systematic errors. Note that thermotropic transitions are not exclusive to pure lipid membranes or proteins, the cooperativity during the transitions is long known to extend over domains or proto-mers consisting of both proteins and lipids(37, 41). Furthermore, ΔI_n have been measured for thermotropic transitions in membranes and proteins induced by a variety of thermodynamic fields including temperature(36, 39, 42), pressure(40), as well as pH(37). Thus, the term "thermotropic transition" is employed in the most general sense, which is indicated by a nonlinearity or cooperativity in the functional relationship between the thermodynamic variables. For example, by observing nonlinearities in I_{2930} as a function of pH and temperature in erythrocytes ghosts, others have previously concluded that ΔI_{2930} represents a "concerted process at apolar protein-lipid boundaries"(37, 38).

Therefore, ΔI_{2930} in figure 1 shows that the membrane essentially undergoes a concerted condensation during voltage-clamped depolarisation. That is, just like temperature, pressure, and pH; membrane potential can also induce a thermotropic transition in the membrane. Furthermore, based on observed ΔI_{2930} in figure 1 the extent of freezing can also be estimated. For example, (I_{2930}/I_{2850}) changes from 1.9 at $-60mV$ (resting potential) to 1.6 at $+30mV$ (depolarised), i.e. ~18% change. In model membranes, transitions can be very steep, $(FWHM\ (C_p) \approx 2\ ℃)$(43), and an equivalent change in spectrum is observed for $\Delta T \approx -2\ ℃$.(30) On the other hand, heat capacity peak in biological membranes can be up to 10 times wider $(FWHM\ (C_p) \approx 20\ ℃)$(16). Hence, to obtain equivalent ΔT corresponding $I_n(T)$ needs to be measured in neuronal membranes. Temperature dependence of Raman spectra has been measured previously in a variety of neuronal membranes(44, 45). For example, in unmyelinated garfish olfactory nerve, the ratio (I_{2950}/I_{2885}) was measured as a function of temperature. The ratio changes from 1.22 at $25\ ℃$ to 1.09 at $6\ ℃$, i.e. 12% change over $\Delta T = 19\ ℃$, which as discussed in detail by the authors, represents a significant increase in order. On the other hand, based on the SRS study in primary neurons by Lee and Cheng(35), (I_{2950}/I_{2885}) changes from 1.18 at $-60mV$ (resting potential) to 1.04 at $+30mV$ (depolarised), i.e. 13% change, which is consistent with a $\Delta T \approx 20\ ℃$ as expected from the $FWHM\ (C_p) \approx 20\ ℃$, in general, in biological membranes. Thus unlike other optical observables measured previously, where the sign of the signal could not be interpreted in absolute terms, a negative ΔI_{2930} has an absolute meaning which indicates freezing.

Using these numbers, we estimate the enthalpy of phase change as well as average heat capacity of neuronal membranes from $I_n(T)$ using the Van't Hoff's approximation (46) and equilibrium constant defined in terms of Raman intensities (47);

$$\frac{dlnK}{dT} = \frac{\Delta H}{RT^2} \tag{4}$$

$$\frac{\Delta K}{K} \approx \frac{\Delta(I_{2950}/I_{2885})}{(I_{2950}/I_{2885})} \tag{5}$$

A 12% change in (I_{2950}/I_{2885}) over $\Delta T = 19\ ℃$ gives an average $\Delta H \approx 4.5\ kJ/mol$ and $c_P = 224 Jmol^{-1}K^{-1}$. These values are now employed to estimate state changes during an action potential.

State changes during an action potential

Can the analysis be extended to state changes during an action potential? Raman spectroscopy has a long history of determining dynamic state changes within propagating wavefronts in fields like thermos-fluids(48–50). While the above discussion assumed equilibrium during voltage clamp, eq. (2) can be extended to an arbitrary macroscopic state (partial equilibrium)(33); by observing region so small that the corresponding relaxation time ($\approx l/c$, l is the length of the region, and c is the speed of sound in the medium) is smaller than the fastest timescale of interest in the underlying process. SRS signal (fig. 2) obtained previously during an action potential in a single neuron satisfies these criteria and showed $\Delta I_{2930} \approx -1\%$ upon depolarisation and $\Delta I_{2930} \approx +1\%$ upon hyperpolarisation during an action potential. These changes confirm concerted freezing and melting of the membrane during the action potential.

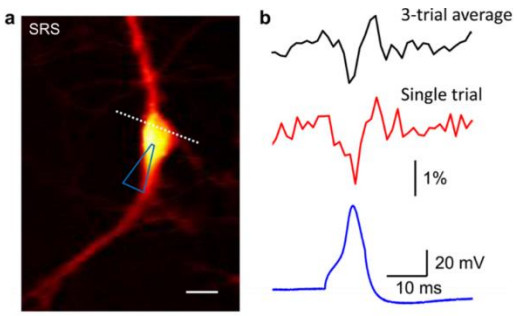

Figure 2. (a) SRS image of a patched neuron. The dashed line indicates the scanning trace. (b) 3-trial average (black) and single-trial SRS time trace (red) of the neuron shown in panel a with simultaneous current clamp recording (blue), showing a single action potential. The SRS intensity was normalized by the SRS reference generated with the same pulses. Scale bar: 20 μm. Reprinted (adapted) with permission from (J. Phys. Chem. Lett. 2017, 8, 9, 1932-1936). Copyright (2017) American Chemical Society

Note that unlike the voltage-clamp experiments where the temperature is constant, there is no such requirement during an action potential, which represents a fundamentally different thermodynamic process. To compare the two, recall that there are quantities that can remain constant even during such dynamic process, most well-known being the entropy that remains constant, for example, during the propagation of sound waves. The entropy production due to dissipation is a second-order effect, hence even in dissipative medium sound waves are assumed to be isentropic to first order(51). Furthermore, the observed temperature changes during a nerve impulse indicate a substantially reversible phenomenon, which led to the original suggestion that nerve impulse or action potentials emerge from the same underlying physics as sound waves(12).

Relation to the thermodynamics of compression waves and fluctuations

So if the state changes during an action potential are indeed similar to those that might occur during sound waves, how do we reconcile (i) the membrane freezes, while (ii) the temperature increases, (iii) the entropy remains constant, and (iv) channel activity increases? Critical insights on this matter have been generated by studying 2D compression waves and fluctuations in artificial lipids films.

Let us first consider the compression waves. Remarkably, near an order-disorder transition in a lipid film, these waves show many key characteristic properties of action potentials including all-or-none excitation(15, 19) and annihilation upon collision(20). In the case of artificial lipid films, the characteristics emerge naturally from the underlying thermodynamic state changes. The picture that has emerged is plotted in figure 3. Note how the phase transition region can be traversed differently at a constant temperature, constant entropy, or constant pressure.

Consider the initial state of the membrane represented by (T_0S_0), then $\Delta I_{2930} \approx -9\%$ during the voltage clamp represents condensation along a constant temperature path $(T = T_0)$, while $\Delta I_{2930} \approx -1\%$ during the action potential represents condensation along constant entropy path $(S = S_0)$.

Therefore, the competition between the condensing effect of the electromechanical compression of the membrane and the fluidizing effect of the increase in temperature due to the release of latent heat is determined by the inclination of the co-existence region in the TS diagram, a parameter known as retrogradicity(15, 52). Another way to interpret the behaviour is in terms of heat capacity; if the heat capacity of a material is sufficiently high, the temperature rise due to the latent heat (released during condensation) will be small enough for the system to still condense under compression. For example, water vapour does not condense upon adiabatic compression. On the other hand, polymers with chain lengths greater than 4 carbon atoms, typically show retrograde behaviour and condense upon adiabatic compression ($c_P > \sim 200 Jmol^{-1}K^{-1}$).(53)

Therefore, the observed $\delta I_{2930}(t)$ has thermal as well as electromechanical contributions that can be estimated to first order using;

$$\delta I_{2930}(t)_{heat\ corrected} = \delta I_{2930_V} + \delta I_{2930_T} \quad (6)$$

$$\delta I_{2930_T} \approx \left(\frac{\partial I_n}{\partial T}\right) \delta T \quad (7)$$

$$\delta I_{2930_V} \approx \left(\frac{\partial I_n}{\partial V}\right) \delta V \quad (8)$$

To evaluate these equation we make following assumptions; (i) the resting state is close to the phase boundary, (ii) due to latent heat contributions ΔH is assumed large compared to state changes that do not involve a phase change, (iii) $\delta V(t)$ is assumed to span the phase change region completely, i.e. the fraction of membrane in condensed phase, $\alpha = 0$ at $\delta V(t) = -60mV$ and $\alpha = 1$ at $\delta V(t) = 30mV$, (iv) $\Delta H_{fluid \rightarrow condensed}{}_{adiabatic} = \beta \Delta H_{fluid \rightarrow condensed}{}_{isobaric}$, where is β is a phenomenological parameter < 1 as adiabatic phase change is closer to the apex of the coexistence dome (enthalpy of transition decreases as the transition temperature approaches critical temperature) and we assume $\Delta H_{fluid \rightarrow condensed}{}_{isobaric} = 4.5\ kJ/mol$, i.e. the estimate obtained above. With these assumptions we get;

$$\delta I_{2930_T}(t) \approx \left(\frac{\partial I_n}{\partial T}\right) \frac{\alpha(t)\beta}{c_p} \Delta H_{fluid \rightarrow condensed}{}_{isobaric} \quad (9)$$

$$\alpha(t) = \frac{\delta V(t) - 60}{90} \quad (10)$$

$\delta I_{2930}(t)_{heat\ corrected}$ thus calculated is plotted in figure3 for $\beta = 0.4$. As shown the measured $\delta I_{2930_T}(t)$ is recovered from the voltage clamp data after accounting for the latent heat during an adiabatic phase change. It is interesting to note that during the rising phase the estimated and observed $\delta I_{2930}(t)$ align correctly, the recovery in measured $\delta I_{2930}(t)$ occurs before the recovery of $\delta I_{2930_V}(t)$ indicating that membrane relaxation occurs before the recovery in voltage.

That the orientation of dipoles in the membrane changes was long known through an extensive range of studies, however a change in dipole orientation is necessary but not sufficient to conclude an increase in order(25, 54). For that, changes in both the magnitude and the distribution of an observable are required as indicated by eq. (2). Few previous studies have performed such experiments on nerves however a corresponding thermodynamic interpretation was not provided. For example, measurements of difference in infrared spectra between resting and excited state of nerve bundles from several species indicated changes in the conformation of membrane phospholipids(55). Similarly, Raman peaks of carotenoids(56) in the membrane during an action potential indicated compression of the molecules, however, whether the compression corresponds to freezing could not be inferred. Tasaki et.al. measured the difference in the emission spectrum between the resting and excited state of solvatochromic fluorescent dyes(57). While the observed blue shift indicated an increase in order, the recent thermodynamic interpretation of the spectral width of these dyes(34) confirmed that an increase in order was indeed observed in Tasaki's experiments. However, given the uncertainty regarding the specific environment of dyes, doubts remained. Similarly, an order-disorder transition during an action potential has been indicated by the measurements of membrane-fluidity sensitive dyes(58).

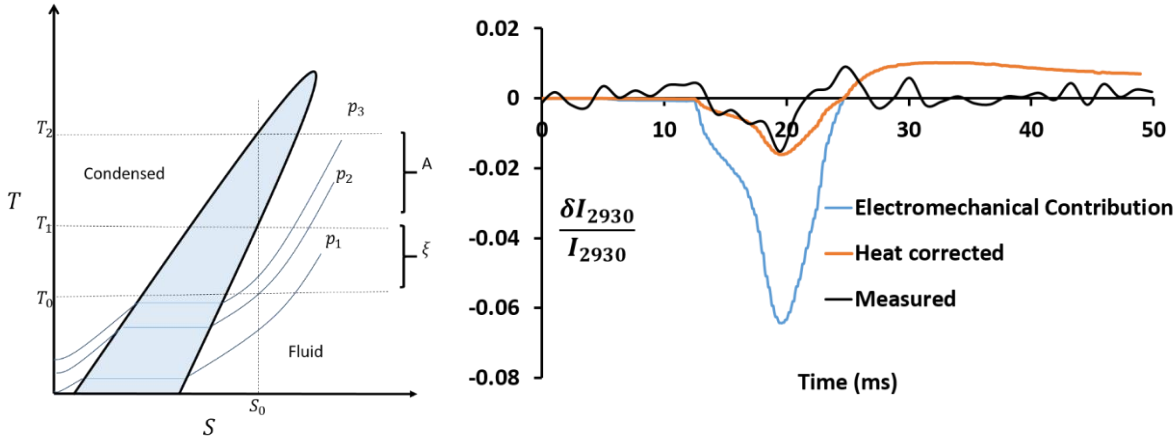

Figure 3. (Left) TS diagram as an aid to the eye, informed by experiments in artificial lipid films(15, 59)*. The hypothesized transition region is shaded. The region makes an acute angle with S axis for retrograde materials. Assuming that complete phase change takes place across the wavefront where the system is always in local equilibrium during an impulse, starting at* $(T_0 S_0)$*, the process across the wavefront is represented by the isentrope* $S = S_0$*. The threshold and amplitude scale with* ξ *and A respectively, i.e. the distance between the initial state and the intersection of the isentrope with the phase boundary. Different isobars* p_i *have been overlaid where* $p_3 > p_2 > p_1$*. (Right) Purely electrochemical component* $\delta I_{2930_V}(t)$*(blue curve) estimated from voltage clamp experiments (from fig.1), is overlaid on calculated heat corrected curve* $\delta I_{2930}\,(t)_{heat\ corrected}$*, and measured* $\delta I_{2930}\,(t)$ *(from fig.2)*

Finally, a brief comment on the nature of fluctuations during the process which relates to channel activity during an action potential. Here, ΔI_{2930} represents first-order changes in the state during an action potential. However, fluctuations represent second-order changes, which have been proposed as the basis for the regulation of channels current (60–63) in the thermodynamic approach and can be accessed by measuring the second order changes $\Delta\Delta I_{2930}$, e.g. by resolving changes in the width of the peak(26). The relation between fluctuation and temperature includes a material constant (see eq. (2) and eq. (3)), like heat capacity or

compressibility (in general known as thermodynamic susceptibilities). Usually, susceptibilities are taken to be "constants" and fluctuations are assumed to be a function of temperature alone. However, the assumption breaks down near a phase transition where heat capacity and compressibility of the membrane have large peaks(16). As the membrane freezes, it goes through this intermediate peak in susceptibility (metastable states), which will increase fluctuations that should cause a spike in channel currents. Such transitions have also been referred as pseudocritical transitions in lipid membranes. Direct evidence of such a role of channel currents during an action potential remains to be seen.

In conclusion, SRS measurements for the first time confirms a long-held belief that the membrane undergoes reversible freezing and melting during an action potential(1, 11, 12, 64, 65). Such changes are consistent with the behavior of two-dimensional compression waves recently observed in artificial lipid films(19). At least in the case of artificial lipid films, the characteristics emerge naturally from the underlying thermodynamic state changes. Now, SRS provides a powerful technique with the spatio-temporal resolution required to investigate action potentials in single neurons as thermodynamic phenomena(1, 12, 14, 19).

References

1. Tasaki, I. 1982. Physiology and electrochemistry of nerve fibers. .

2. Hodgkin, A.L., and A.F. Huxley. 1952. A quantitative description of membrane current and its application to conduction and excitation in nerve. *J. Physiol.* 117:500–544.

3. Tasaki, I. 1995. Mechanical and thermal changes in the Torpedo electric organ associated with its postsynaptic potentials. *Biochem. Biophys. Res. Commun.* 215:654–658.

4. Cohen, L.B., B. Hille, and R.D. Keynes. 1969. Light scattering and birefringence changes during activity in the electric organ of Electrophorus electricus. *J. Physiol.* 203:489–509.

5. Conti, F., and I. Tasaki. 1970. Changes in extrinsic fluorescence in squid axons during voltage-clamp. *Science (80-.).* 169:1322–1324.

6. Barry, J.F., M.J. Turner, J.M. Schloss, D.R. Glenn, Y. Song, M.D. Lukin, H. Park, and R.L. Walsworth. 2016. Optical magnetic detection of single-neuron action potentials using quantum defects in diamond. *Proc. Natl. Acad. Sci.* 113:14133–14138.

7. Howarth, J. V, and R.D. Keynes. 1975. The heat production associated with the passage of a single impulse in pike olfactory nerve fibres. *J. Physiol.* 249:349–368.

8. El Hady, A., and B.B. Machta. 2015. Mechanical surface waves accompany action potential propagation. *Nat. Commun.* 6:6697.

9. Landau, L.D., and E.M. Lifshitz. 1987. Shock Waves. In: Sykes J, W Reid, editors. Fluid Mechanics. Pergamon Press Ltd. pp. 327–329.

10. Hodgkin, A.L. 1964. The conduction of the nervous impulse. VII. Liverpool: Liverpool University Press.

11. Margineanu, D.-G., and E. Schoffeniels. 1977. Molecular events and energy changes during the action potential. *Proc Natl Acad Sci U S A.* 74:3810–3813.

12. Kaufmann, K. 1989. Action Potentials and Electrochemical Coupling in the Macroscopic Chiral Phospholipid Membrane. *Caruara, Brazil (https://sites.google.com/site/schneiderslab/research-group/literature).*

13. Fox, D. 2018. The Brain, Reimagined. *Sci. Am.* 318:60–67.

14. Heimburg, T., and A.D. Jackson. 2005. On soliton propagation in biomembranes and nerves. *Proc. Natl. Acad. Sci. U. S. A.* 102:9790–9795.

15. Shrivastava, S., K. Kang, and M.F. Schneider. 2015. Solitary Shock Waves and Adiabatic Phase Transitions Lipid Interfaces and Nerves. *Phys. Rev. E*. 91:12715.

16. Mužić, T., F. Tounsi, S.B. Madsen, D. Pollakowski, M. Konrad, and T. Heimburg. 2019. Melting transitions in biomembranes. *Biochim. Biophys. Acta - Biomembr*. 1861:183026.

17. Melchior, D.L., and J.M. Steim. 1976. Thermotropic transitions in biomembranes. *Annu. Rev. Biophys. Bioeng.* 5:205–238.

18. Albrecht, O., and H. Gruler. 1978. Polymorphism of phospholipid monolayers. *J. Phys.* 39:301–324.

19. Shrivastava, S., and M.F. Schneider. 2014. Evidence for two-dimensional solitary sound waves in a lipid controlled interface and its implications for biological signalling. *J. R. Soc. Interface*. 11:1–23.

20. Shrivastava, S., K.H. Kang, and M.F. Schneider. 2018. Collision and annihilation of nonlinear sound waves and action potentials in interfaces. *J. R. Soc. Interface*.

21. Kappler, J., S. Shrivastava, M.F. Schneider, and R.R. Netz. 2017. Nonlinear fractional waves at elastic interfaces. *Phys. Rev. Fluids*.

22. Cohen, L.B., and B.M. Salzberg. 1978. Optical measurement of membrane potential. *Rev. Physiol. Biochem. Pharmacol.* 83:35–88.

23. Einstein, A. 1909. On the Present Status of the Problem of Radiation. *Ann. Phys.* 10:183–195.

24. Einstein, A. 1910. Theory of the Opalescence of homogenous fluids and liquid mixtures near the critical state. *Ann. Phys.* 33:1275–1295.

25. Shrivastava, S., and M.F. Schneider. 2013. Opto-Mechanical Coupling in Interfaces under Static and Propagative Conditions and Its Biological Implications. *PLoS One*. 8:2005–2007.

26. Shrivastava, S., R.O. Cleveland, and M.F. Schneider. 2018. On measuring the acoustic state changes in lipid membranes using fluorescent probes. *Soft Matter*.

27. Raman, C. V. 1928. Nature 121 (March 31, 1928) 501-502 - A new type of scecondary radiation.pdf. *Nature*. 501–502.

28. Schultz, Z.D., and I.W. Levin. 2011. Vibrational spectroscopy of biomembranes. *Annu. Rev. Anal. Chem. (Palo Alto. Calif).* 4:343–366.

29. Hazel, J.R., S.J. McKinley, and M.F. Gerrits. 1998. Thermal acclimation of phase behavior in plasma membrane lipids of rainbow trout hepatocytes. *Am. J. Physiol. - Regul. Integr. Comp. Physiol.* 275:861–869.

30. Gaber, B.P., P. Yager, and W.L. Peticolas. 1978. Interpretation of biomembrane structure by Raman difference spectroscopy. Nature of the endothermic transitions in phosphatidylcholines. *Biophys. J.* 21:161–176.

31. Kaufmann, K. 1989. On the role of the phospholipid membrane in free energy coupling. *Caruaru, Brazil https://sites.google.com/site/schneiderslab/research-group/literature*.

32. Shrivastava, S., and R.O. Cleveland. 2019. Thermodynamic state of the interface during acoustic cavitation in lipid suspensions. *Phys. Rev. Mater.* 3:55602.

33. Landau, L.D., and E.M. Lifshitz. 1980. Entropy for Nonequilibrium. In: Statistical Physics. Burlington,MA: Butterworth-Heinemann. pp. 26–27.

34. Shrivastava, S., R.O. Cleveland, and M.F. Schneider. 2018. On measuring the acoustic state changes in lipid membranes using fluorescent probes. *Soft Matter*.

35. Lee, H.J., D. Zhang, Y. Jiang, X. Wu, P.Y. Shih, C.S. Liao, B. Bungart, X.M. Xu, R. Drenan, E. Bartlett, and J.X. Cheng. 2017. Label-Free Vibrational Spectroscopic Imaging of Neuronal Membrane Potential. *J. Phys. Chem. Lett.* 8:1932–1936.

36. Gaber, B.P., P. Yager, and W.L. Peticolas. 1978. Interpretation of biomembrane structure by Raman difference spectroscopy. Nature of the endothermic transitions in phosphatidylcholines. *Biophys. J.* 21:161–176.

37. Verma, S.P., and D.F.H. Wallach. 1976. Erythrocyte membranes undergo cooperative, pH sensitive state transitions in the physiological temperature range: Evidence from Raman spectroscopy. *Proc. Natl. Acad. Sci. U. S. A.* 73:3558–3561.

38. Verma, S.P., and D.F.H. Wallach. 1977. Changes of Raman scattering in the CH-stretching region during thermally induced unfolding of ribonuclease. *Biochem. Biophys. Res. Commun.* 74:473–479.

39. Levin, I.W., E. Keihn, and W.C. Harris. 1985. A Raman spectroscopic study on the effect of cholesterol on lipid packing in diether phosphatidylcholine bilayer dispersions. *BBA - Biomembr.* 820:40–47.

40. Yager, P., and W.L. Peticolas. 1982. The kinetics of the main phase transition of aqueous dispersions of phospholipids induced by pressure jump and monitored by raman spectroscopy. *BBA - Biomembr.* 688:775–785.

41. Changeux, J.-P., J. Thiery, Y. Tung, and C. Kittel. 1967. ON THE COOPERATIVITY OF BIOLOGICAL MEMBRANES. *Proc. Natl. Acad. Sci.* 57:335–341.

42. Fox, C.B., G.A. Myers, and J.M. Harris. Temperature-Controlled Confocal Raman Microscopy to Detect Phase Transitions in Phospholipid Vesicles. .

43. Koynova, R., and R.C. MacDonald. 2003. Mixtures of cationic lipid O-ethylphosphatidylcholine with membrane lipids and DNA: phase diagrams. *Biophys. J.* 85:2449–2465.

44. Savoie, R., M. Pigeon-Gosselin, M. Pézolet, and D. Georgescauld. 1986. Effect of the action potential on the Raman spectrum of the pike olfactory nerve. *Biochim. Biophys. Acta - Biomembr.* 854:329–333.

45. Pézolet, M., and D. Georgescauld. 1985. Raman spectroscopy of nerve fibers. A study of membrane lipids under steady state conditions. *Biophys. J.* 47:367–372.

46. Holzwarth, J. 1989. Structure and dynamic of phospholipid membranes from nanoseconds to seconds. In: Cooper A, J Houben, L Chien, editors. The Enzyme Catalysis Process Energetics, Mechanism and Dynamics. New York: Springer Science + Buisness Media, LLC. pp. 383–410.

47. Yellin, N., and I.W. Levin. 1977. Cooperative unit size in the gel-liquid crytalline phase transition of dipalmitoyl phosphatidylcholine-water multilayers: An estimate from raman spectroscopy. *BBA - Biomembr.* 468:490–494.

48. Ramos, A., B. Maté, G. Tejeda, J.M. Fernández, and S. Montero. 2000. Raman spectroscopy of hypersonic shock waves. *Phys. Rev. E.* 62:4940–4945.

49. Nagao, H., A. Matsuda, K.G. Nakamura, and K. Kondo. 2003. Nanosecond time-resolved Raman spectroscopy on phase transition of polytetrafluoroethylene under laser-driven shock compression. *Appl. Phys. Lett.* 83:249–250.

50. and, J.M.W., and Y.M. Gupta*. 1997. Shock-Induced Chemical Changes in Neat

Nitromethane: Use of Time-Resolved Raman Spectroscopy. .

51. Lifshitz, L.D.L. and E.M. 1987. Second Viscosity. In: Sykes J, W Reid, editors. Fluid Mechanics. Pergamon Press Ltd. p. 308.

52. Kim, Y.G., G.C. Carofano, and P. a. Thompson. 1986. Shock waves and phase changes in a large-heat-capacity fluid emerging from a tube. *J. Fluid Mech.* 166:57–92.

53. Thompson, P.A., and Y.G. Kim. 1983. Direct observation of shock splitting in a vapor-liquid system. *Phys. Fluids*. 26:3211–3215.

54. Cohen, L.B., and B.M. Salzberg. 1978. Optical measurement of membrane potential. *Rev. Physiol. Biochem. Pharmacol.* 83:35–88.

55. Sherebrin, M.H., B.A.E. MacClement, and A.J. Franko. 1972. Electric-Field-Induced Shifts in the Infrared Spectrum of Conducting Nerve Axons. *Biophys. J.* 12:977–989.

56. Maksimov, G. V, A.A. Churin, V.Z. Paschenko, and A.B. Rubin. 1990. Raman Spectroscopy of the “Potential Sensor” of Potential-Dependent Channels. .

57. Tasaki, I., E. Carbone, K. Sisco, and I. Singer. 1973. Spectral analyses of extrinsic fluorescence of the nerve membrane labeled with aminonaphthalene derivatives. *BBA - Biomembr.* 323:220–233.

58. Georgescauld, D., and H. Duclohier. 1978. Transient fluorescence signals from pyrene labeled pike nerves during action potential possible implications for membrane fluidity changes. *Biochem. Biophys. Res. …*. 85:1186–1191.

59. Shrivastava, S. 2018. Detonation of shock-waves and action potentials in lipid interfaces. In: Proceedings of Meetings on Acoustics. .

60. Micol, V., P. Sánchez-Piñera, J. Villalaín, a de Godos, and J.C. Gómez-Fernández. 1999. Correlation between protein kinase C alpha activity and membrane phase behavior. *Biophys. J.* 76:916–927.

61. Seeger, H.M., L. Aldrovandi, A. Alessandrini, and P. Facci. 2010. Changes in single K(+) channel behavior induced by a lipid phase transition. *Biophys. J.* 99:3675–3683.

62. Fenimore, P.W., H. Frauenfelder, B.H. McMahon, and F.G. Parak. 2002. Slaving: solvent fluctuations dominate protein dynamics and functions. *Proc. Natl. Acad. Sci. U. S. A.* 99:16047–16051.

63. Wunderlich, B., C. Leirer, A. Idzko, U.F. Keyser, A. Wixforth, V.M. Myles, and T. Heimburg. 2009. Phase-State Dependent Current Fluctuations in Pure Lipid Membranes. *Biophysj*. 96:4592–4597.

64. Kobatake, Y., I. Tasaki, and A. Watanabe. 1971. Phase transition in membrane with reference to nerve excitation. *Adv. Biophys.* 2:1–31.

65. Inoue, I., Y. Kobatake, and I. Tasaki. 1973. Excitability, instability and phase transitions in squid axon membrane under internal perfusion with dilute salt solutions. *BBA - Biomembr.* 307:471–477.